



Proceedings of the Eighteenth International Conference on
Civil, Structural and Environmental Engineering Computing
Edited by: P. Iványi, J. Kruis and B.H.V. Topping
Civil-Comp Conferences, Volume 10, Paper 2.1
Civil-Comp Press, Edinburgh, United Kingdom, 2025
ISSN: 2753-3239, doi: 10.4203/ccc.10.2.1
©Civil-Comp Ltd, Edinburgh, UK, 2025

Adjusting the Parameters of the Three-Layer Track Model to Suppress the Negative Influence of the Critical Velocity

Z. Dimitrovova^{1,2}

**¹Institute of Mechanical Engineering, Instituto Superior Técnico,
Lisboa, Portugal**

**²Department of Civil Engineering, Nova School of Science and
Technology, NOVA FCT, Caparica, Portugal**

Abstract

This paper gives indications for the rail track design in order to allow train circulation at high speeds. This is demonstrated on a three-layer model of the railway track. This model should exhibit three critical velocities for resonance, however, very often the lowest value is replaced by the so-called pseudocritical velocity. The aim of this paper is therefore to tailor the geometry and material parameters of this model to provide properties leading to a significant reduction of the influence of the pseudocritical velocity so that only a slight increase in vibrations is detected. It is then possible to extend the range of traffic speeds to very high values without compromising the circulation safety. This is very important for the current trends of increasing the speed and capacity of the railway network.

Keywords: three-layer model, integral transforms, semianalytical methods, critical velocity, moving loads, onset of instability.

1 Introduction

Environmental issues are of utmost importance nowadays. Closely related to this is the necessity to switch from road to rail transport and increase the capacity of the railway network. One way to increase the capacity of the network can be achieved by increasing the speed of travel, but excessive speed is related to the safety and comfort of passengers. Travelling speed is naturally limited by the critical velocity. The definition of the critical velocity is not unambiguous but usually corresponds to the lowest velocity of wave propagation in the railway track. Mathematically, it is defined

as the velocity for resonance, because when a constant force moves along the track at the critical velocity, then in the absence of damping, the deflections tend to infinity.

The critical velocity for resonance can be accurately determined on numerical models. Detailed finite element models are frequently used, however reduced and simplified models offer a sufficient approximation to reality combined with computational efficiency, as has been demonstrated in classical works [1,2]. The possibility of certain simplifications has been also analysed by other researchers [3], the pyramid model has been extended and renamed as the stress cone theory in [4,5], where suitable formulas for estimating the characteristics of the three-layer model are given. This has been further refined, and additional confirmation of the adequacy is given in [6] for a wide range of possible mechanical and geometrical specifications related to the detailed finite element model.

In simplified models such as layered models [1,2,5] consisting of a guide beam and supported by a set of point masses connected by spring-damper elements, this calculation can be performed in the Fourier domain by identifying at least one real-valued double pole on the Fourier variable axis. Then under such conditions the result of the inverse Fourier transform tends to infinity. It has been shown that this resonance is not always present [7]. Considering a three-layer model, there should be five resonances, three of which can be named as the true critical velocity and two of which as the false critical velocity. It is important to perform the evaluation by analytical approaches, since numerical approaches cannot clearly distinguish a sharp peak from a resonance. For example, the frequently used Green's function method needs damping for numerical stability to perform the numerical integration of a time series, [8]. In the presence of damping, the true resonance is never clear, a sharp peak may occur, but it is not certain that without damping the displacement would be infinite. If there is no true resonance, the term pseudocritical velocity should be used. The pseudocritical velocity can be determined by parametric analysis, but when it is not very well pronounced, then its value is ambiguous because the maximum may be located at different velocities for a maximum or minimum over the entire structure, or for the peak at the active point.

The critical velocity for resonance is related to the moving force problem, which means that the load corresponds to a single constant force moving at a constant velocity over the structure. Then the transient part of the solution is not important, and the steady-state part can be solved directly. In the case of a true critical velocity, there are infinite displacements at the critical velocity, but for an infinitely larger velocity, the displacement at the active point is zero. This fundamental characteristic is not verified for pseudo or false critical velocities. The pseudocritical velocity is characterised by an increase in vibrations, but all deflections are always finite. No zero at the active point is observed for infinitely larger velocity. The false critical velocity is characterized by infinite displacements like a true resonance, but again no zero at the active point is observed for infinitely larger velocity. As for the connection to the instability of a single moving mass, then the real and pseudocritical velocities are associated with it, but not the false critical velocity. In fact, the pseudocritical

velocity replaces the true one when resonance is mathematically impossible and always indicates the lowest value.

2 The Model and its Parameters

The model considered in this paper is shown in Figure 1. It is characterised by a guiding beam described by its bending stiffness EI and mass per unit length m . The supporting structure is composed of point masses: m_s (half sleeper mass) and m_b (dynamically activated ballast mass) and spring-damper elements (k_p and c_p - stiffness and damping coefficients of the rail pads; k_b and c_b - stiffness and damping coefficients of the dynamically activated ballast mass; and k_f and c_f - stiffness and damping coefficients of the foundation). In addition, k_s denotes the shear stiffness. While m_s , m_b , k_p , c_p , k_b , c_b and k_s are usually given in discrete form, k_f and c_f are already distributed over the length.

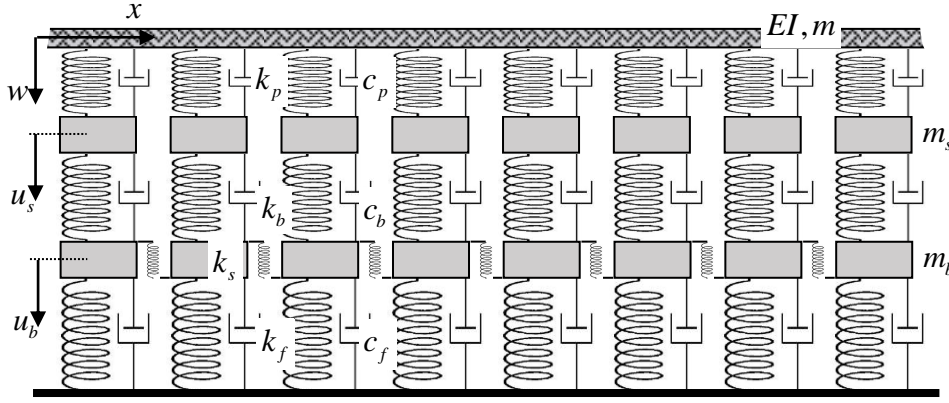


Figure 1: Three-layer model of the railway track.

To facilitate the analytical steps of the solution, all parameters are introduced into the governing equations in their distributed form. The sleeper spacing l_s is used to change the discrete parameters to their distributed counterparts. For convenience and ease of calculation, the model is finally described by a set of dimensionless parameters, the basis of which is the guiding beam on the Winkler foundation described by k_f and c_f .

It has been shown that in most cases the pseudocritical velocity can alternatively be determined as the velocity at the vertical asymptote to the instability line determined for a one moving mass problem. To do this, one can choose infinitesimal damping, and an infinitesimal real-valued frequency and determine in a semianalytical manner the velocity for an infinitely large moving mass. However, there are cases where this asymptote does not exist, but the pseudocritical velocity does.

These cases are characterized by a very small increase in vibrations, thus opening the way to extend the travel speed into the supercritical region. To select the most advantageous cases, some criteria need to be established. First of all, the increase in upward displacement, which is the most detrimental, must be as low as possible, and

the next resonant velocity or onset of instability for some realistic value of the moving mass must be as high as possible.

This paper establishes guidelines on how to identify and find the most advantageous cases so that by careful combination of them the lowest pseudocritical velocity is barely visible and can be exceeded. The aim is therefore not to push the critical velocity to higher values, but to make it negligibly detrimental so that it can be overpassed.

The allowable ranges of admissible mechanical parameters characterizing the rail track have been roughly summarized in [8], however, it should be noted that these ranges are still flexible, because of the current tendency of enlarging the spacing between sleepers, [9,10] or using new and lightweight materials. The reference beam is assumed in form of a guiding Euler-Bernoulli beam standing for the rail supported by a Winkler foundation and it is known that a very wide range of values can be found in the literature for this foundation stiffness [11,12]. However, within these ranges it is not possible to consider all possible combinations, as will be explained in the next section.

3 Methods

First, a set of parameters for describing the reference beam needs to be defined:

$$\chi = \sqrt[4]{\frac{k_f}{4EI}}, \quad v_{ref} = \sqrt[4]{\frac{4k_f EI}{m^2}} = \frac{1}{\chi} \sqrt{\frac{k_f}{m}}, \quad \alpha = \frac{v}{v_{ref}} \quad (1)$$

where χ is inverse of the characteristic length, v_{ref} is the critical velocity of the reference beam and α is used for the velocity ratio. The main parameters describing the three-layer model are two mass ratios and two stiffness ratios:

$$\mu_s = \frac{m_s}{l_s m}, \quad \mu_b = \frac{m_b}{l_s m}, \quad \kappa_p = \frac{k_p}{l_s k_f}, \quad \kappa_b = \frac{k_b}{l_s k_f} \quad (2)$$

Additional parameters express the shear stiffness and damping ratios:

$$\eta_s = \frac{k_s l_s}{2\sqrt{EI k_f}}, \quad \eta_p = \frac{c_p}{2l_s \sqrt{m k_f}}, \quad \eta_b = \frac{c_b}{2l_s \sqrt{m k_f}}, \quad \eta_f = \frac{c_f}{2\sqrt{m k_f}} \quad (3)$$

Then, even if the range of parameters has been established in [8] as:

$$\mu_s \in \langle 1; 6 \rangle, \quad \mu_b \in \langle 2; 45 \rangle, \quad \kappa_p \in \langle 0.03; 4.2 \times 10^4 \rangle, \quad \kappa_b \in \langle 0.04; 6 \times 10^3 \rangle \quad (4)$$

It is clear from Equation (2) that

$$0.015 \leq \frac{\kappa_p}{\kappa_b} \leq 126.58, \quad 0.022 \leq \frac{\mu_s}{\mu_b} \leq 2.05 \quad (5)$$

using the base values used for determination of the ranges in Equation (4).

Next, test cases have been selected to analyse what characteristics can lead to the desirable situation. One of the selected cases is characterized by $\mu_s=3$ and $\mu_b=10$. Stiffness parameters are better characterized on a logarithmic scale, since for very

high values, indicators such as resonance and others become insensitive to any alterations. With this in mind, the following designation is introduced:

$$\kappa_p = 0.03 \times 10^{0.05(ind_p-1)}, \quad \kappa_b = 0.04 \times 10^{0.05(ind_b-1)} \quad (6)$$

With such defined ind_p and ind_b , running from 1 to 101, the values covered are:

$$\kappa_p \in \langle 0.03; 3000 \rangle, \quad \kappa_b \in \langle 0.04; 4000 \rangle \quad (7)$$

For the test case $ind_b=20$ and 63 has been selected. Then, the interesting part of the graphs, shown in Figure 2, is contained up to $ind_p=51$.

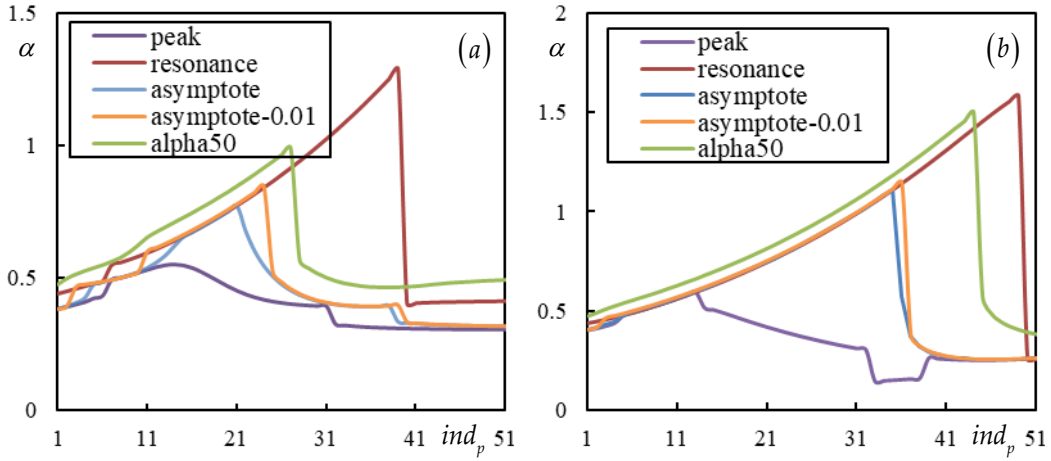


Figure 2: Analysis of the tested case: $\mu_s = 3$, $\mu_b = 10$: (a) $ind_b = 20$; (b) $ind_b = 63$.

It is important for the analysis to establish how to read the graphs in Figure 2. First, the purple line indicates the velocity ratio at which the first peak is detected in upward displacements. These calculations are performed using the undamped steady-state solution. Since the minimum value is taken from the entire beam, to ensure an accurate value without unnecessarily analysing too long a part of the beam, in order to provide an exact value without unnecessary analysis of excessively long part of the beam, the roots of the characteristic equation are divided in a way that the propagating and evanescent waves are dealt with separately, and the function envelope is determined for the propagating part. The purple curve thus indicates the probable location of the pseudocritical velocity and should be smooth. However, sometimes there are step differences between adjacent velocities. This is caused by two facts: first – the peak is not fully developed, and therefore a second peak is actually indicated; second – there is a premature small peak that is not dominant and cannot replace the pseudocritical velocity. Distinguishing such cases may be important for the definition of some characteristic performance index, however, after choosing the optimal case, parametric analysis can confirm its effectiveness. However, for further purposes, this value is denoted as pseudocritical, α_{PCV} .

The red curve indicates the lowest true resonance, α_{res} . This value is determined analytically. As already mentioned, the deflections for such a velocity tend to infinity,

and therefore such an occurrence should be as far away from α_{PCV} as possible. The blue and orange curves are used for the lowest asymptote to the first branch of an instability line. The difference is that the blue curve is calculated for negligible damping and the orange one for a realistic but low damping of 1% for all levels, that is $\eta_p=\eta_b=\eta_f=0.01$. There are some differences, but not very significant. Finally, the green curve marks the lowest velocity for which instability occurs for the moving mass ratio $\eta_M=50$, α_{m50} . The dimensionless moving mass ratio is defined as:

$$\eta_M = \frac{M\chi}{m} \quad (8)$$

where M is the moving mass value. This curve additionally shows whether the instability indicated by one of the asymptotes can represent a real danger, because, very often the first instability branch indicates unreasonably high η_M . The optimal case is then defined as the case where the increase in upward displacements at the first peak \tilde{w}_{\min}^{PCV} relative to the static downward displacement \tilde{w}_{st} is as low as possible and at the same time the first resonance or instability for $\eta_M=50$ is as far away from the first peak as possible; whichever occurs first is decisive. Therefore, the performance index is defined as:

$$PI = \frac{|\tilde{w}_{\min}^{PCV}|}{\tilde{w}_{st}} + \frac{1}{100 \min \left(\frac{\alpha_{res} - \alpha_{PCV}}{\alpha_{PCV}}, \frac{\alpha_{m50} - \alpha_{PCV}}{\alpha_{PCV}} \right)} \quad (9)$$

where dimensionless displacement is defined as:

$$\tilde{w} = \frac{w}{w_{ref}} \quad \text{with} \quad w_{ref} = \frac{P\chi}{2k_f} \quad (10)$$

In Equation (10) w_{ref} is the static displacement on the reference beam and P is the applied force.

4 Results

By careful analysis of the PI in the test cases, the minimum values for the two $ind_b=20$ and 63 have been found to be 1.385 and 0.076, respectively. The latter result is due to a premature peak and should be disregarded, the valid value is then 0.541. Several attempts have been made to run an optimization analysis, but due to the time required to fully analyse the test cases, a statistical analysis was performed. The response surface was determined for several cases; however, the optimal values were always located on its boundary and the predictions for the interior values were therefore compromised. One such case is shown in Figure 3. This case is characterized by $\mu_s=4$, $\mu_b=12$, $ind_b=40$ and $\eta_s=0$. The optimal $PI=0.496$ is obtained for $ind_p=16$. It can be seen that α_{res} precedes α_{m50} (vertical line IN50) and is therefore decisive for the PI value. The increase in the upward displacements at α_{PCV} is barely visible. This case indicates that the critical velocity can be overpassed by 44%, indicating a significantly expanded range for circulation velocities.

To reduce the optimization time, careful analysis revealed that the most likely cases of significant improvements are those where the difference between α_{res} within the range of admissible ind_p is the largest. Such calculations can only be preformed in software with high number of digits precision, therefore this criterium was applied on α of the lowest asymptote for the moving mass problem at $\eta_p=\eta_b=\eta_f=0.01$, which can be run very quickly in Matlab.

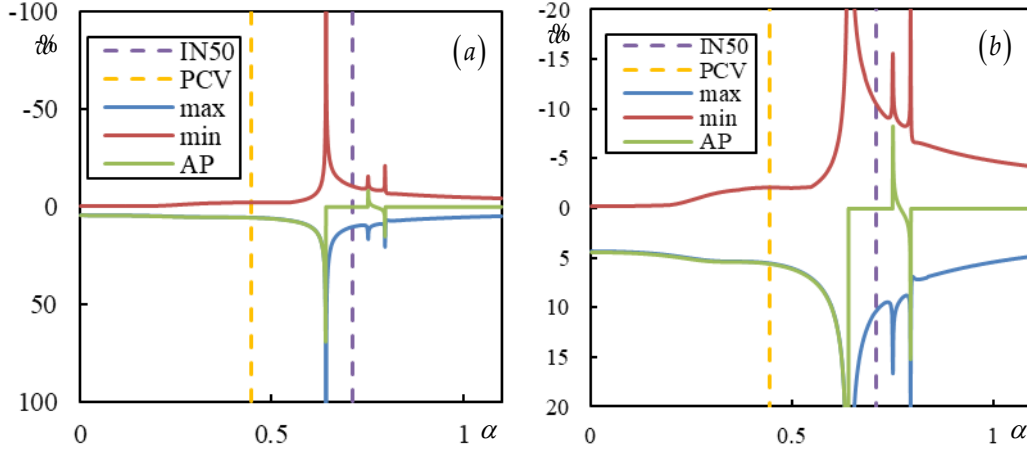


Figure 3: Parametric analysis of the tested case: $\mu_s = 4$, $\mu_b = 12$, $ind_b = 40$ and $\eta_s = 0$: (a) enlarged vertical scale; (b) reduced vertical scale.

A Monte Carlo simulation was performed, but by performing three independent runs with a large number of loops, several repeated results were detected indicating that the ‘rand’ function is vulnerable to using same values instead of exploring the full interval. The results for the optimal case, where the difference in values was 88.89% are shown in Figure 4.

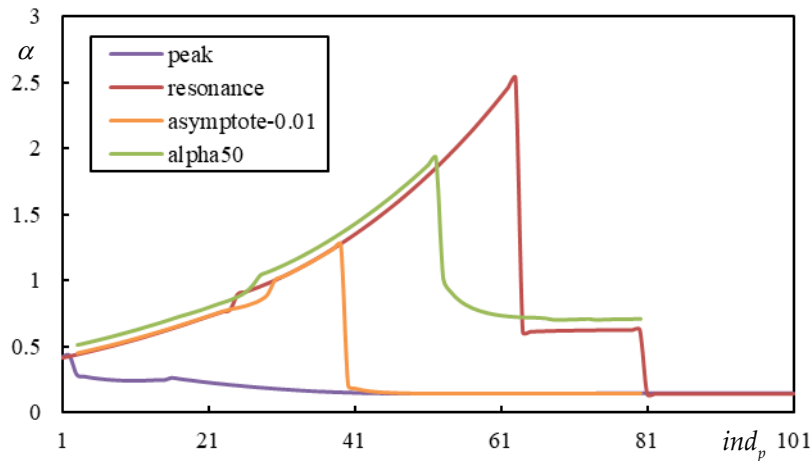


Figure 4: Optimum case from Monte Carlo simulation: $\mu_s = 5.524$, $\mu_b = 44.129$, $\kappa_b = 44.887$, $\eta_s = 0.111$.

A detailed analysis of the optimal case allowed for selection of the optimal $PI=0.175$. Unfortunately, this is an unrealistic case, because it is obtained for $ind_p=7$, leading to the ratio between stiffnesses of 0.0096, which is outside the allowable interval. Assuming $ind_p=11$, the ratio between stiffnesses is already acceptable, and the PI is still quite low, 0.190. The parametric analysis of these cases is reported in Figures 5 and 6. In the latter case, an even higher increase beyond α_{PCV} is possible, 132,5% until the first resonance, instead of 99.0%, but the increase in upward displacements is slightly higher, which leads to a worse PI .

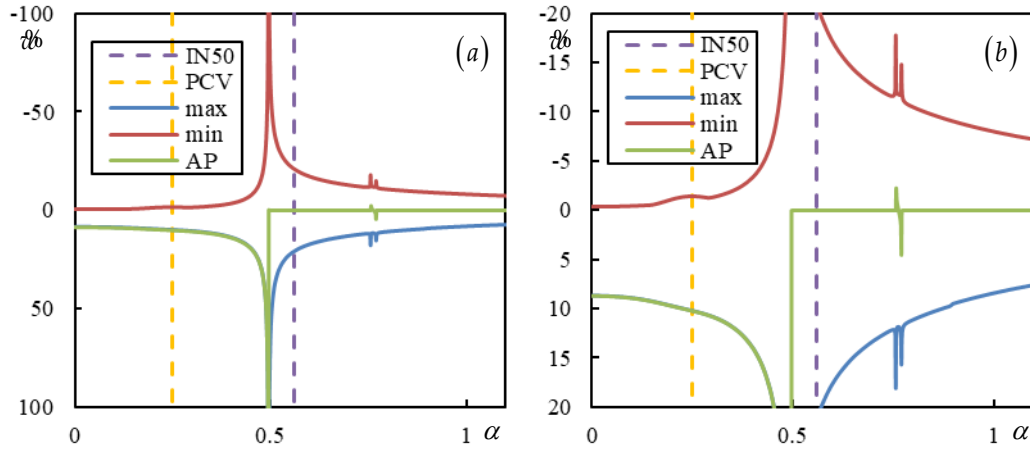


Figure 5: Parametric analysis of the optimal case: $\mu_s = 5.524$, $\mu_b = 44.129$, $\kappa_b = 44.887$, $\eta_s = 0.111$, $ind_p = 7$: (a) enlarged vertical scale; (b) reduced vertical scale.

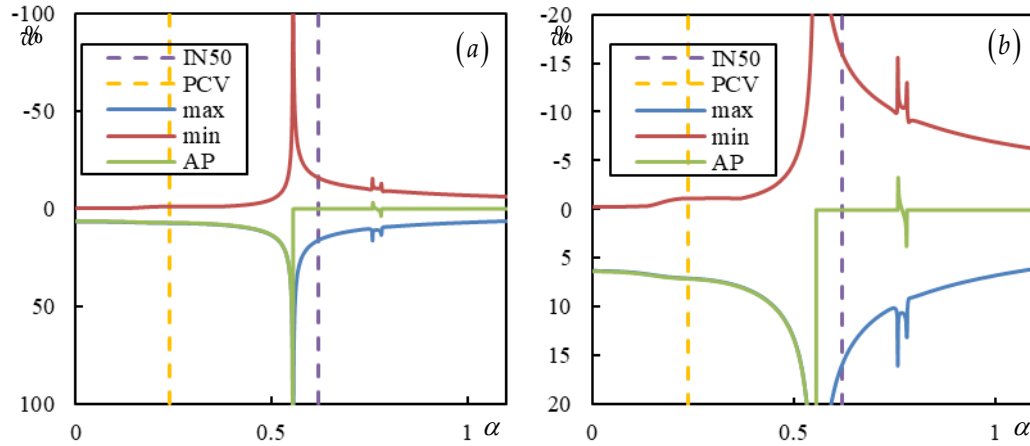


Figure 6: Parametric analysis of the optimal case: $\mu_s = 5.524$, $\mu_b = 44.129$, $\kappa_b = 44.887$, $\eta_s = 0.111$, $ind_p = 11$: (a) enlarged vertical scale; (b) reduced vertical scale.

Regarding the determination of realistic values for the track design, it is important to point out that each of these cases can cover a large range of possible scenarios. It is just possible to define some possible ranges for the definition of the ballast layer and then search within the best options for the ratios of stiffness and mass parameters within the ranges defined in Equation (5).

5 Conclusions and Contributions

This paper presents guidelines for optimizing the geometric and material parameters of railway tracks in order to increase circulation speeds above the critical velocity without compromising safety and comfort. It was shown that significant increases, on the order of 132%, can be achieved. This analysis is performed on a three-layer railway track model, which is generally accepted by other researchers as an adequate model, combining computational efficiency with reasonable relevance to real-world situations. Several analyses and techniques have been tested to see how to effectively predict the optimal case.

Acknowledgements

The author acknowledges Fundação para a Ciência e a Tecnologia (FCT) for its financial support via the project LAETA Base Funding (DOI: 10.54499/UIDB/50022/2020).

References

- [1] S.L. Grassie, R.W. Gregory, D. Harrison, K.L. Johnson, “The dynamic response of railway track to high frequency vertical excitation”, *Journal of Mechanical Engineering Science*, 24(2), 77-90, 1982.
- [2] K.L. Knothe, S.L. Grassie, “Modelling of railway track and vehicle-track interaction at high frequencies”, *Vehicle System Dynamics*, 22, 209–262, 1993.
- [3] K. Nguyen, J.M. Goicolea, F. Galbadon, “Comparison of dynamic effects of high-speed traffic load on ballasted track using a simplified two-dimensional and full three-dimensional model”, *Proceedings of the Institution of Mechanical Engineers, Part F: Journal of Rail and Rapid Transit*, 228, 128–142. 2014.
- [4] W. Zhai, Z. Cai, “Dynamic interaction between a lumped mass vehicle and a discretely supported continuous rail track”, *Computers and Structures*, 63, 987–997, 1997.
- [5] M.W. Zhai, K.Y. Wang, J.H. Lin, “Modelling and experiment of railway ballast vibrations”, *Journal of Sound and Vibration*, 270, 673–683, 2004.
- [6] A.S.F. Rodrigues, Z. Dimitrovová, “Applicability of a three-layer model for the dynamic analysis of ballasted railway tracks”, *Vibration*, 4, 151-174, 2021.
- [7] Z. Dimitrovová, “On the critical velocity of moving force and instability of moving mass in layered railway track models by semianalytical approaches”, *Vibration*, 6, 113-146, 2023.
- [8] Z. Dimitrovová, T. Mazilu, “Semi-Analytical Approach and Green’s Function Method: A Comparison in the Analysis of the Interaction of a Moving Mass on an Infinite Beam on a Three-Layer Viscoelastic Foundation at the Stability

- Limit—The Effect of Damping of Foundation Materials”, *Materials*, 17, 279, 2024.
- [9] R. Sañudo, M. Miranda, B. Alonso, V. Markine, “Sleepers spacing analysis in railway track infrastructure”, *Infrastructures*, 7, 83, 2022.
 - [10] R.S. Ortega, J. Pombo, S. Ricci, M. Miranda, “The importance of sleepers spacing in railways”, *Constr. Build. Mater.* 300, 124326, 2021.
 - [11] K.N. Van Dalen, *Ground Vibration Induced by a High-Speed Train Running over Inhomogeneous Subsoil, Transition Radiation in Two-Dimensional Inhomogeneous Elastic Systems*. Master’s Thesis, Department of Structural Engineering, TUDelft, Delft, The Netherlands, 2006.
 - [12] Y.-H. Chen, Y.-H. Huang, C.-T. Shih, “Response of an Infinite Timoshenko Beam on a Viscoelastic Foundation to a Harmonic Moving Load”, *Journal of Sound and Vibration*, 241, 809–824, 2001.